Applied Physics A (2025) 131:115
https://doi.org/10.1007/s00339-024-08227-7

Self-assembly of Ag NWs on the surface of modified grating PDMS film for flexible SERS sensors

Xinshuo Liu[1] · Youchang Long[1] · Lei Huang[1] · Guina Xiao[1]

Received: 8 October 2024 / Accepted: 27 December 2024 / Published online: 17 January 2025

Abstract
Flexible Raman-enhanced substrates possess the advantages of good adsorbability and extensibility, which are particularly beneficial for the effective analyses of target molecules on complex or irregular surfaces. Here, we reported a large-scale, flexible and transparent surface-enhanced Raman scattering (SERS) substrate. This Ag NWs/M-CDG/PDMS substrate was composed of a modified compact disc grating polydimethylsiloxane (M-CDG/PDMS) film decorated with silver nanowires (Ag NWs) through a self-assembly process. The surface of the grating PDMS film was modified with 3-aminopropyltriethoxysilane (APTES) to create a hydrophilic layer. The contact angle of the APTES-modified PDMS film decreased from 105° to 66°, indicating improved hydrophilicity compared to the unmodified film. Thiram was chosen as a probe molecule to evaluate the SERS performance of the prepared substrates. It was found that the substrate displayed high SERS sensitivity with a detection limit for thiram as low as 10^{-8} M, and good uniformity, evidenced by RSD (relative standard deviation) values of 8.7% and 9.9%. Moreover, the fabricated substrate showed good mechanical stability and SERS enhancement effects even under backlight illumination, making it suitable for in-situ SERS detection on curved surfaces. The Ag NWs/M-CDG/PDMS flexible substrate also demonstrated the advantages of anti-corrosion, mixed detection capabilities, a wide operating temperature range, and the ability to perform vapor phase detection. In summary, the developed Ag NWs/M-CDG/PDMS substrate had great potential for practical applications in detection technologies.

Keywords Surface-enhanced Raman scattering · Patterned PDMS film · Silver nanowires (Ag NWs) · Self-assembly · Thiram

1 Introduction

Surface-enhanced Raman scattering (SERS) exhibits characteristics of excellent sensitivity, rapid detection and strong anti-interference [1], which has been widely used in environmental monitoring, food safety, and medical hygiene [2–4]. It is generally accepted that the SERS enhancement arises from the excitation of localized surface plasmon resonance (LSPR) in adjacent plasmonic nanostructures [5], resulting in the formation of intense electromagnetic fields with narrow nanogaps named "hot spots" [6]. Therefore, designing suitable plasmonic nanostructures to construct SERS substrate with a high-density of "hot spots" is essential for achieving high-performance SERS detection.

Noble metallic nanostructures [7] have been engineered as highly sensitive SERS substrate due to the strong intensity generated between localized surface nanoarrays, where the "hot spots" provided significant electromagnetic field enhancement [8]. Materials like gold [9], silver [10] and copper [11] are often utilized for this purpose. According to the SERS enhancement mechanism, silver is considered as the preferred SERS material. For instance, Zhang et al. [12] developed a reinforced hydrogel by reduction of plasmonic silver nanoparticles (Ag NPs) on a PNIPAM membrane using polyvinylpyrrolidone (PVP) as a surfactant. Lee et al. [13] studied the efficiency of surface-enhanced Raman spectroscopy (SERS) through the oblique angle deposition of Ag with different deposition rates and substrates. The majority of SERS substrates are based on rigid silicon [14, 15] or glass [16]. However, the inflexibility of these substrates limits their applicability for in-situ detection [17] on

✉ Guina Xiao
xiaoguina@shnu.edu.cn

[1] Department of Physics, Shanghai Normal University, Shanghai 200234, P.R. China

non-planar or curved surfaces. To overcome this limitation, the development of flexible and transparent SERS substrates with rapid and easy-to-operate characteristics have become a hot topic. Such substrates can enable conformal contact with curved surfaces and facilitate in-situ detection. At present, various materials that combine desirable flexibility with optical transparency are available for this purpose. These include polyethylene terephthalate (PET) [18], polydimethylsiloxane (PDMS) [19], poly(methyl methacrylate) (PMMA) [20], and poly-vinyl chloride (PVC) [21]. Among them, PDMS is particularly favored as a base for SERS substrate because of its flexible, excellent stability, good adsorption and high transparency [22]. A patterned PDMS film can provide uniform and high-density "hot spots", while also increasing the surface area, thereby improving spectral enhancement.

Patterned PDMS film [23] was obtained by using a template-assisted method, wherein the compact disc grating (CDG) served as a template to replicate the grating structure onto the PDMS surface. This approach was not only straightforward but also enabled the high-throughput, low-cost preparation of large-area nanopatterns. Various metal nanostructures have been fabricated on substrates through techniques such as magnetron sputtering [24], ion beam sputtering [25], inkjet printing [26] and self-assembly [27]. However, methods like magnetron sputtering and ion beam sputtering have high requirements for objective factors. In contrast, self-assembly is recognized as a low-cost strategy. The successful preparation of Ag NWs/M-CDG/PDMS substrate relied on integrating silver nanowires (Ag NWs) [28] with the modified compact disc grating PDMS film (M-CDG/PDMS). The modification principle involved grafting amino group onto the surface of the grating PDMS film to change its wettability [29] through APTES treatment [30]. After modification, an increased density of Ag NWs could be arranged on the surface of grating PDMS film, thereby enhancing its SERS performance significantly.

In this study, silver nanowires were deposited on the modified grating PDMS substrate through self-assembly. The surface of the grating PDMS substrate was modified with APTES treatment to create a hydrophilic layer, thereby enhancing the adhesion of silver nanowires (denoted as Ag NWs/M-CDG/PDMS). By utilizing self-assembly, the deposition of Ag NWs led to the formation of numerous "hot spots". Optimizing the diluted ratio of Ag NWs resulted in a prepared Ag NWs/M-CDG/PDMS substrate that exhibited high SERS activity, good uniformity, and mechanical stability. Using thiram as a probe molecule, the substrate also possessed anti-interference properties, enabling it to perform hybrid detection. Additionally, the developed substrate was successfully applied for the vapor phase detection of thiram.

2 Experimental

2.1 Materials

A compact disc (CD 700 MB, 5 inches) was purchased from Sony. Silver nanowires (Ag NWs) were purchased from Zhejiang Kechuang Advanced Materials Technology Co., Ltd. 3-aminopropyltriethoxysilane (APTES, 97% purity) was sourced from Beijing Bailingwei Technology Co., Ltd. Polydimethylsiloxane (PDMS) was sourced from Dow Corning Europe Limited. Analytical grade reagent thiram (99.99% purity) and malachite green (MG) were purchased from Shanghai National Pharmaceutical Group Chemical Reagent Co., Ltd.

2.2 Preparation of Ag NWs/M-CDG/PDMS substrate

As illustrated in Fig. 1, the process started by removing the protective and reflective layers from the compact disc, exposing the underlying grating structure. The processed compact disc were then ultrasonically cleaned for 10 min and allowed to air dry naturally. Next, the PDMS prepolymer was combined with the curing agent at a weight ratio of 10:1 and thoroughly mixed for 20 min. The mixture was then left to stand for 30 min to eliminate any bubbles. This bubble-free mixture was coated onto the clean surface of the grating compact disc and subjected to thermal curing at 100 °C for 30 min. After curing, the PDMS film was peeled off from the compact disc and cut into 3×3 cm^2 pieces. This procedure resulted in the transfer of the grating structure onto the PDMS film surface. Subsequently, these grating PDMS films were immersed in a modification solution (C_2H_5OH: DI: APTES = 95:3:2, v/v) at 70 °C for 2 hours. Finally, a series of diluted solutions of silver nanowires were self-assembled onto the surface of grating PDMS film at room temperature (approximately 25°C) for 24 h, leading to the successful development of Ag NWs/M-CDG/PDMS substrate.

2.3 Characterization

The as-prepared SERS substrates were characterized using a field-emission scanning electron microscope (FESEM S4800). The wettability of the Ag NWs/M-CDG/PDMS substrate was investigated by a contact angle measuring instrument. SERS detection was performed by a laser micro Raman spectrometer (PTT-MRI) at room temperature, with the laser wavelength, power, and integration time of 532 nm, 5 mW and 20 s, respectively.

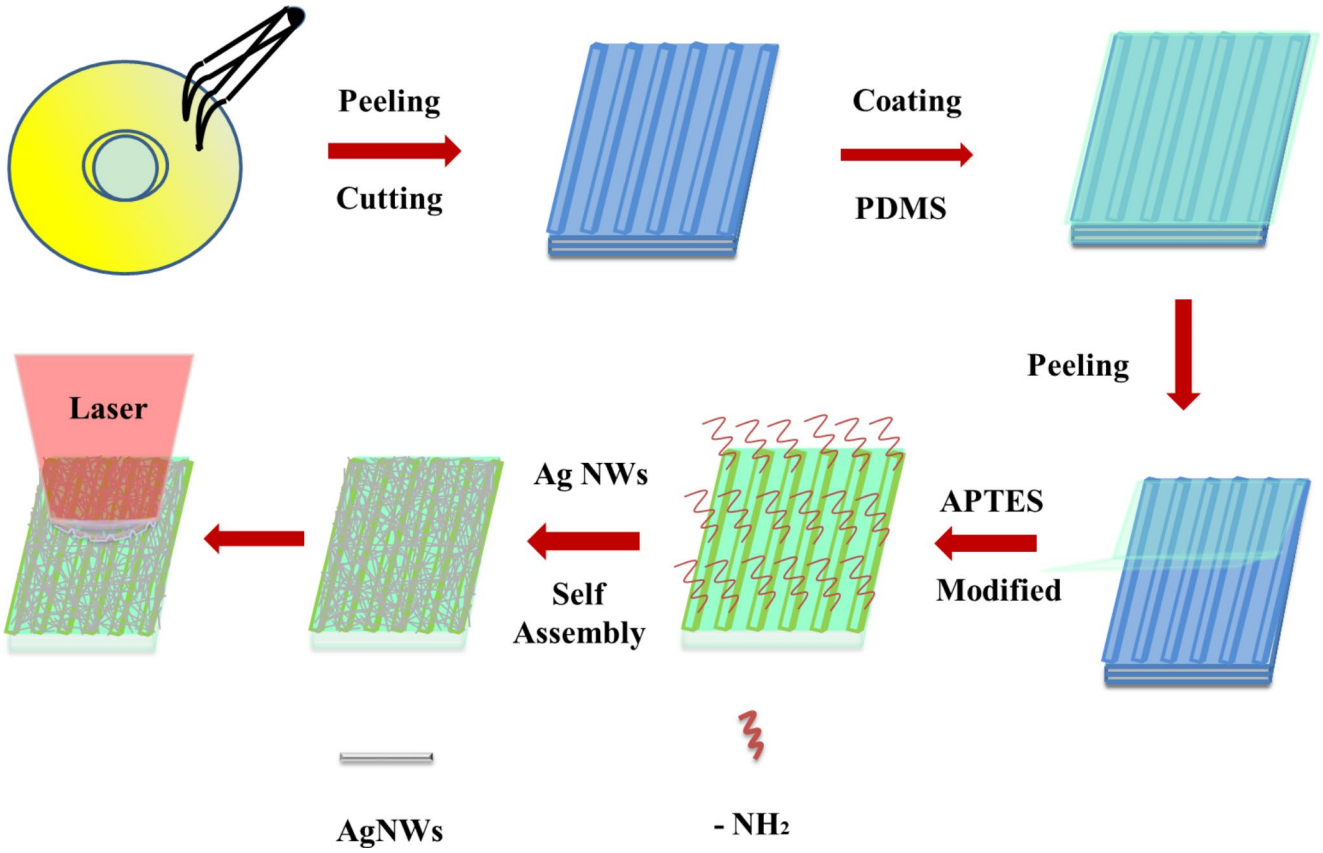

Fig. 1 Developed process of Ag NWs/M-CDG/PDMS substrate

2.4 SERS measurements

To evaluate the SERS sensitivity of Ag NWs/M-CDG/PDMS substrate, 1μL of thiram solution was dropped on the surfaces of fabricated substrates. After drying at room temperature, SERS spectra of thiram were collected from these substrates using a Raman spectrometer. For vapor phase measurements of thiram, 0.01 g of thiram powder was weighed and placed into small beaker. The opening of the beaker was then fully covered with the prepared substrate. The small beaker was subsequently heated for varying durations, and at each interval, SERS measurements were taken using the Raman spectrometer.

2.5 Results and discussion

2.6 Characterization of morphology and structure of Ag NWs/M-CDG/PDMS films

Figure S1a shows that the blank PDMS film possessed good transparency. As observed in Fig. S1b, the grating PDMS film not only retained high transparency but also displayed distinctive colored bands. After modification with APTES, the transparency of the grating PDMS surface was visibly diminished, as demonstrated in Fig. S1c. An interlaced network structure comprised of silver nanowires was evident on the surface of the Ag NWs/M-CDG/PDMS substrate, as depicted in Fig. S1d.

The surface morphologies of the four prepared substrates were investigated by SEM, as presented in Fig. 2. The blank PDMS film possessed a smooth surface devoid of any complex structures, as shown in Fig. 2a. Figure 2b indicated the grating structure on the surface of PDMS film, which is primarily responsible for the light interference effect and the emergence of colored bands. Following modification with APTES, the grating PDMS film still retained its grating structure, however, due to the introduction of amino groups, the clarity of its surface grating structure was reduced, as depicted in Fig. 2c. Figure 2d illustrates the Ag NWs/M-CDG/PDMS film, where the disordered arrangement of silver nanowires formed a loose and porous network on the surface.

To verify the effects of modification and self-assembly on the wettability of the prepared substrate. The wettability of the blank PDMS, CDG/PDMS, M-CDG/PDMS and Ag NWs/M-CDG/PDMS were investigated by a contact angle measuring instrument, as shown in the inset of Fig. 2.

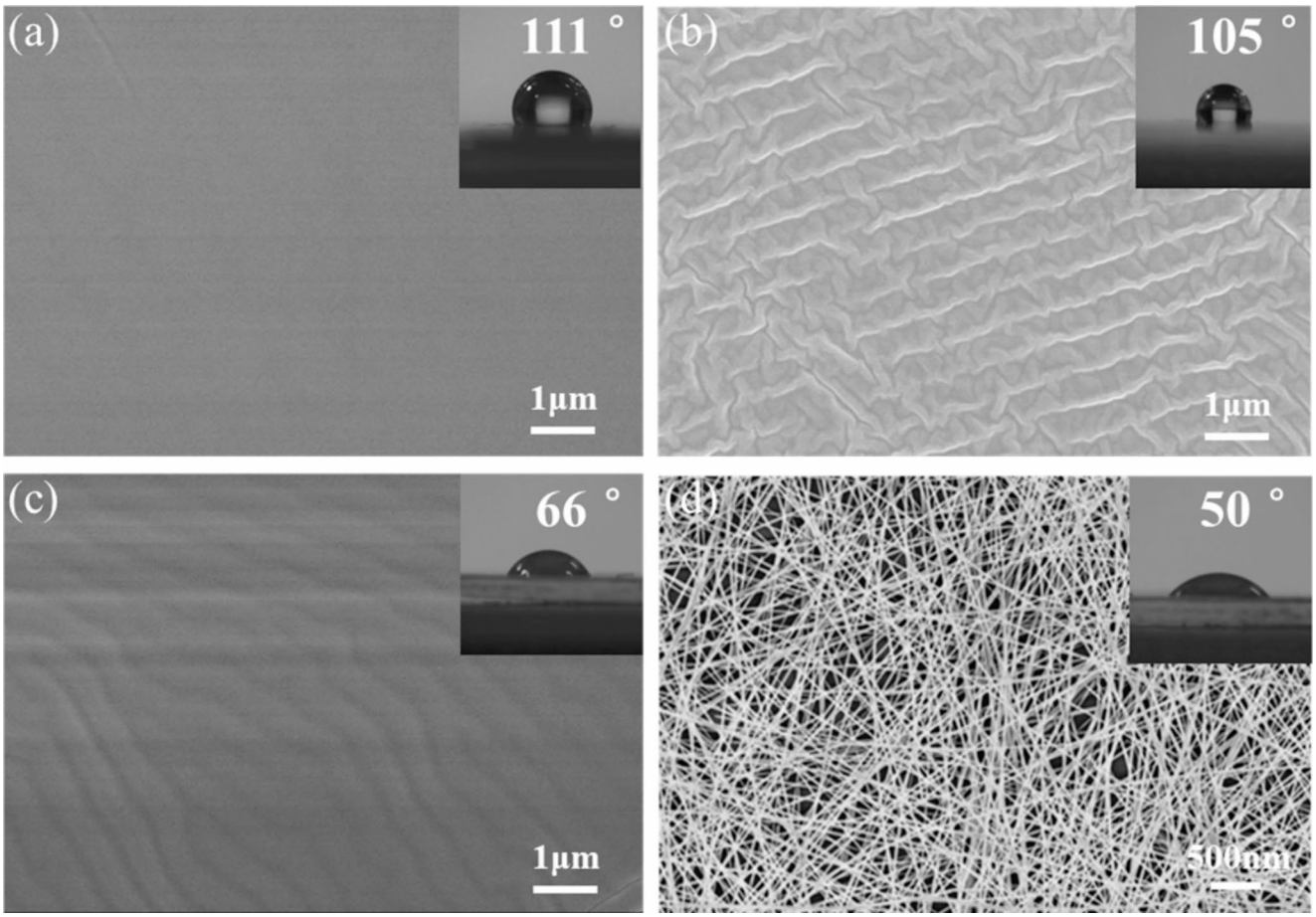

Fig. 2 SEM images of (**a**) blank PDMS film, (**b**) CDG/PDMS film, (**c**) M-CDG/PDMS film, (**d**) Ag NWs/M-CDG/PDMS substrate. The inset showed the corresponding contact angle images

The untreated surface of the blank and grating PDMS films exhibited contact angle of 110° and 105°, respectively. After APTES modification, the value of the contact angle decreased from 105° to 66°, indicating the successful creation of a hydrophilic surface layer on the PDMS film. Subsequent self-assembly further reduced the contact angle to 50°. The results indicated that both the APTES modification and the self-assembly process significantly enhanced the hydrophilicity of the substrates, with the latter also promoting the aggregation of analytes to improve SERS sensitivity.

2.7 Evaluation of SERS performances, uniformity and stability of the prepared substrate

For evaluating the SERS enhancement capability of the four different substrates, 10^{-5} M thiram was chosen as the probing molecule. In Fig. 3a, the Ag NWs/CDG/PDMS substrate exhibited a stronger SERS enhancement effect compared to the Ag NWs/PDMS substrate. When the substrate was modified with APTES, the Ag NWs/M-CDG/PDMS substrate showed an even stronger SERS enhancement effect compared to the Ag NWs/CDG/PDMS substrate. This might be attributed to the strong coupling between localized surface plasmon resonance (LSPR) resulting from the grating structures and the high degree of intersection of Ag NWs. Figure 3b showed the variations in SERS intensity for 10^{-5} M thiram at 1381 cm^{-1} and 1510 cm^{-1} with four different substrates. In a word, the SERS performance of the Ag NWs/M-CDG/PDMS substrate was the best among the four substrates. Therefore, all subsequent experiments were conducted on Ag NWs/M-CDG/PDMS substrate without special instructions.

Self-assembly is one of the most common methods for preparing flexible SERS substrates. One of the critical parameter during this process was the concentration of metallic nanostructures. This factor played a significant role in determining their morphology and distribution on the substrate surface, which in turn had a profound impact on SERS enhancement. Therefore, silver nanowires were deposited on the modified grating PDMS film by regulating the dilution ratio, which facilitated the fabrication and optimization of SERS substrates. Fig. S2 displayed SEM

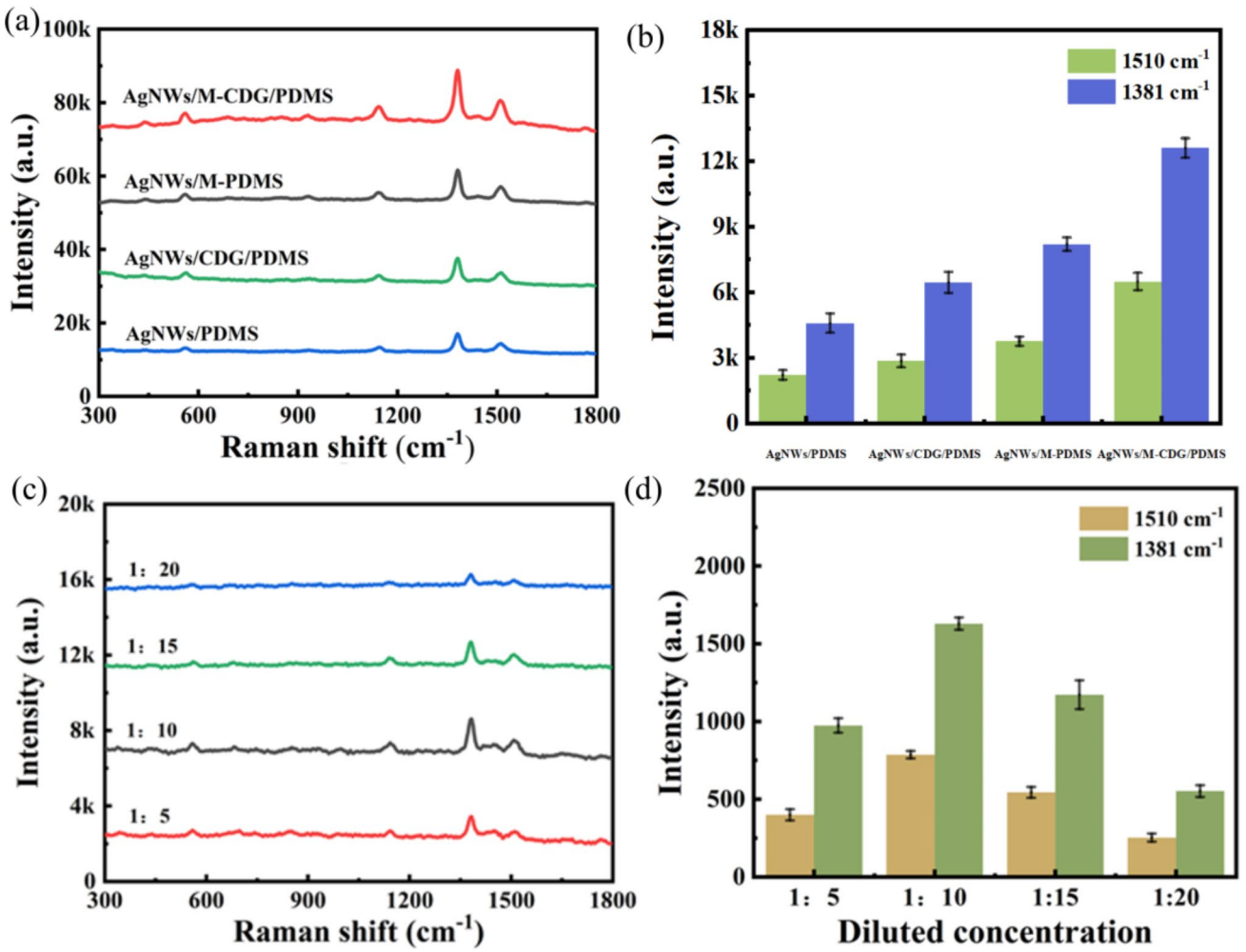

Fig. 3 (**a**) SERS spectra of 10^{-5} M thiram on the four different substrates. (**b**) The corresponding peak intensities of the SERS spectra at 1381 cm^{-1} and 1510 cm^{-1}. (**c**) SERS spectra of 10^{-5} M thiram adsorbed on the prepared substrates at various dilution ratios. (**d**) The corresponding peak intensities of the SERS spectra at 1381 cm^{-1} and 1510 cm^{-1}

images of modified grating PDMS films decorated with Ag NWs at different dilution ratios (Ag NWs: DI v/v) ranging from 1:5 to 1:20 in intervals of 5. It can be seen that the Ag NWs are densely packed, forming a network with a high coverage on the surface at dilution ratios of 1:5 and 1:10. For the dilution ratio of 1:15, gaps between Ag NWs became noticeable. At the highest dilution ratio of 1:20, the lowest density and most significant gaps were observed, indicating much-reduced coverage. To investigate the SERS activities of Ag NWs/M-CDG/PDMS substrates fabricated with different dilution ratios, 10^{-5} M thiram was used as a probe molecule to obtain the SERS spectra, and the result was shown in Fig. 3c. At a lower dilution ratio of 1:5, the coalescence between adjacent Ag NWs reduced the number of gaps, leading to a decrease in the intensity of the SERS signal. As the dilution ratio increased to 1:10, the spacing between neighboring silver nanowires became more pronounced, resulting in an increased number of gaps. This created a higher density of "hot spots" within the Ag NWs network, thereby enhancing the SERS signal intensity. Correspondingly, the SERS signal intensity increased. However, at higher dilution ratios (1:15 and 1:20), the quantity of Ag NWs become insufficient, failing to adequately cover the modified grating PDMS layer, thus leading to a diminution in the SERS signal intensity. In addition, Fig. 3d clearly illustrated the trend of SERS intensity at 1381 cm^{-1} and 1510 cm^{-1} changing with dilution ratio. As the dilution ratio increased from 1:5 to 1:20, leading to a decrease in the concentration of silver nanowires (Ag NWs), the SERS intensity initially increased due to optimal gap formation between Ag NWs, before eventually decreasing as the gaps became less frequent. Therefore, Ag NWs/M-CDG/PDMS substrate with dilution ratio of 1:10 was used in subsequent SERS measurement.

To further confirm the effects of the modification, we compared the SERS signal intensity between the modified

Ag NWs/CDG/PDMS substrate and the unmodified Ag NWs/CDG/PDMS substrate. Under the same conditions (1 μL of thiram solution), the SERS signal intensity from the modified Ag NWs/CDG/PDMS film was significantly higher than that from the unmodified Ag NWs/CDG/PDMS. Moreover, the detection limit for the modified substrate was notably improved, achieving sensitivity to 10^{-8} M thiram solution as shown in Fig. 4b, compared to 10^{-6} M for the unmodified Ag NWs/CDG/PDMS film in Fig. 4a.

Uniformity is a critical parameter for evaluating the reliability of SERS-based quantitative analyses in practical applications. To assess this, the uniformity of the unmodified Ag NWs/CDG/PDMS substrate was evaluated by recording the Raman intensity of 10^{-5} M thiram at 1381 cm^{-1} and 1510 cm^{-1} from 20 randomly selected spots on the surface. The obtained relative standard deviations (RSD) were 19.3% and 26.5%, respectively (Fig. 4c). Similarly, for the modified Ag NWs/CDG/PDMS substrate, the signal homogeneity was examined by acquiring SERS spectra of 10^{-5} M thiram from 20 different spots across the substrate. As shown in Fig. 4d, the RSD values for peak intensities at 1381 cm^{-1} and 1510 cm^{-1} were calculated to be 8.7% and 9.9%, respectively. Which exhibited that the modified Ag NWs/CDG/PDMS substrate possessed the good uniformity. These results indicated that the modified Ag NWs/CDG/PDMS substrate exhibited superior uniformity compared to the unmodified counterpart. Thus, it can be concluded that the modification process significantly enhanced the uniformity of the prepared substrate.

In addition, time stability and repeatability are critical factors in evaluating the performance of SERS substrates. As illustrated in Fig. 5a, the prepared substrate exhibited excellent long-term stability, with its Raman enhancement effect remaining robust throughout the storage period, showing only a slight decrease in signal intensity. Furthermore, as depicted in the Fig. 5b, the signal intensity of thiram molecular layers on 15 different batches of composite substrates was remarkably consistent. This consistency indicated that the composite substrates prepared using our designed method possessed not only good time stability

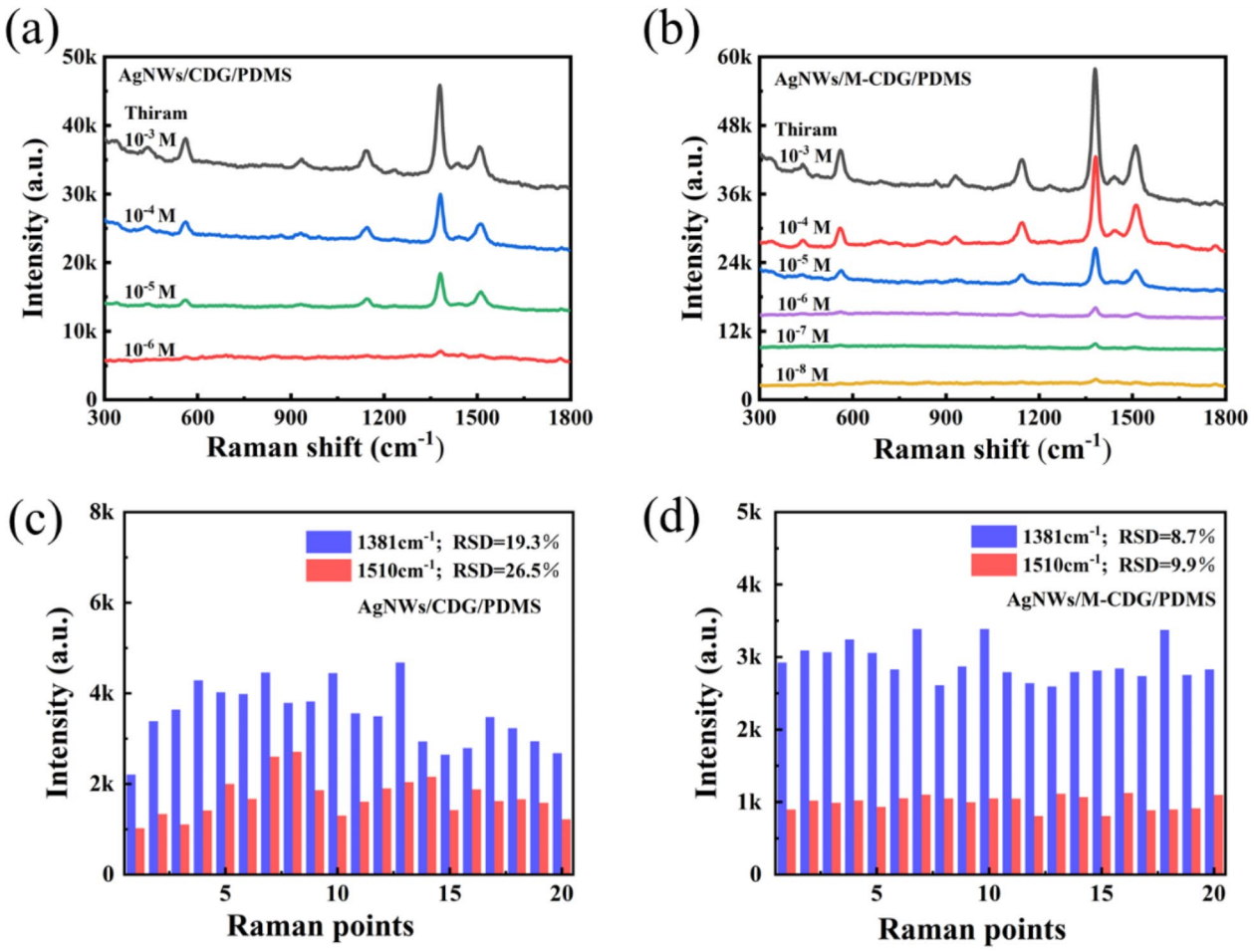

Fig. 4 SERS spectra of thiram with different concentrations on (**a**) Ag NWs/CDG/PDMS substrate, (**b**) Ag NWs/M-CDG/PDMS substrate. (**c-d**) The corresponding peak intensities at 1381 cm^{-1} and 1510 cm^{-1}

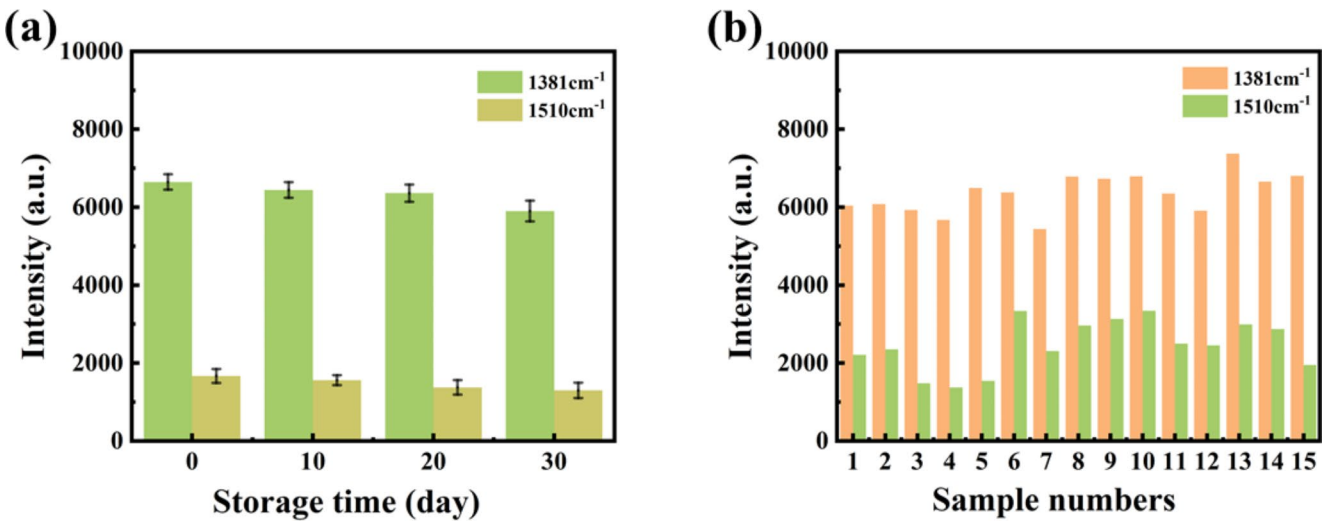

Fig. 5 (**a**) The intensity of the characteristic peaks for thiram at 1381 cm^{-1} and 1510 cm^{-1} as a function of time during storage.(**b**) Bar charts illustrating the peak intensity of SERS signals for 10^{-5} M thiram recorded from 15 different samples at wavenumbers 1381 cm^{-1} and 1510 cm^{-1}

but also high reproducibility. Overall, these results demonstrated the superior qualitative and quantitative reliability of the substrates.

2.8 Mechanical properties of the Ag NWs/M-CDG/PDMS substrate

For practical applications, the mechanical stability of the flexible SERS substrates is also very important. To further assess the influence of mechanical stimuli on the SERS activity of the Ag NWs/M-CDG/PDMS substrate, repeated mechanical deformations, including bending and torsion, were carried out. The substrates were subjected to being bent in half and twisted to 180°, respectively. After every 10 cycles of mechanical stimuli, we collected the SERS signals of 10^{-4} M thiram solution on the substrate to assess its durability performance, as shown in Fig. 6a and b. Similarly, the mechanical stability of the Ag NWs/M-CDG/PDMS substrate was further investigated by collecting the SERS spectra of 10^{-4} M thiram solution and comparing peak intensities at 1381 cm^{-1} performed in bending and twisting tests. Even after 100 cycles of various mechanical deformations, the peak intensity at 1381 cm^{-1} exhibited only negligible changes in comparison to the original state without deformation, as illustrated in Fig. 6c. These results verified that the Ag NWs/M-CDG/PDMS substrates possess good mechanical stability against both bending and twisting because of their excellent flexibility.

Additionally, the adhesion between plasmonic nanostructures and the modified elastomeric film should be tenacious, otherwise the SERS activity will be significantly weakened due to the loss of metallic nanostructures during the SERS measurements. Therefore, the adhesion between the Ag NWs and the modified grating PDMS film was investigated using a scotch tape peel test. Figure 6d depicted the SERS spectra of 10^{-4} M thiram collected on the Ag NWs/M-CDG/PDMS substrate after three peeling cycles. There was negligible variation in SERS intensity at 1381 cm^{-1} (the inset of Fig. 5d), indicating a robust adhesion between the Ag NWs and the modified grating PDMS film. The above results demonstrated that the Ag NWs/M-CDG/PDMS substrate exhibited outstanding mechanical stability, allowing it to easily achieve conformal contact with curved surfaces without impairing SERS performance.

The effect of substrate stretching was performed on the flexible Ag NWs/M-CDG/PDMS substrate measured by 10^{-4} M thiram as the probing molecule (Fig. 6e). The SERS intensity showed a slight decrease as the stretching length increased. Specifically, when the stretching length increased from 0 to 1.2 cm, the SERS intensity decreased by 30–40%, as shown in Fig. 6f.

2.9 Anti-interference testing of the flexible Ag NWs/M-CDG/PDMS substrate

The developed Ag NWs/M-CDG/PDMS flexible substrate not only displayed good SERS sensitivity and stability but also showed anti-corrosion properties, hybrid detection capabilities, and a wide operating temperature range. As evidenced in Fig. 7a, even when exposed to acidic environments (pH = 2) or alkaline conditions (pH = 14), the substrate maintained better Raman signals for thiram at a concentration of 10^{-4} M. Therefore, the prepared substrate was suitable for SERS detection under complex and extreme conditions. To enable the simultaneous detection of different types of pollutants, solutions of thiram and malachite green

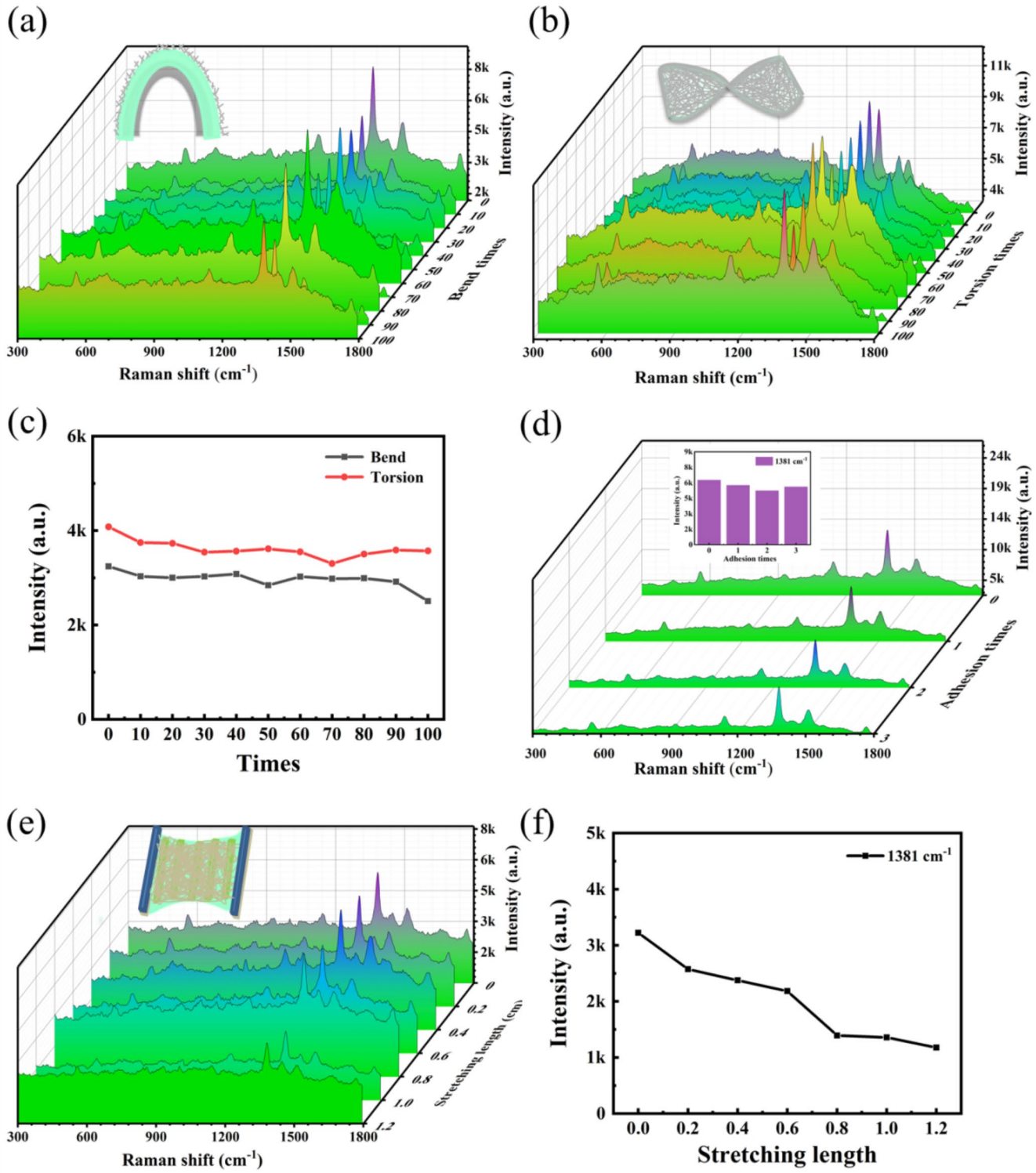

Fig. 6 SERS spectra of thiram detected on the developed substrate under various mechanical conditions: (**a**) bending half, (**b**) torsion to 180°. (**c**) Corresponding signal intensities at 1381 cm^{-1} after bending and torsion. (**d**) Raman spectra from three adhesion tests using scotch tape. The inset showed the SERS intensity at 1381 cm^{-1} as a function of the number of adhesion cycles. (**e**) SERS spectra of the developed substrate after different stretching length (0–1.2 cm). (**f**) Raman intensities at 1381 cm^{-1} after different stretching length (0–1.2 cm)

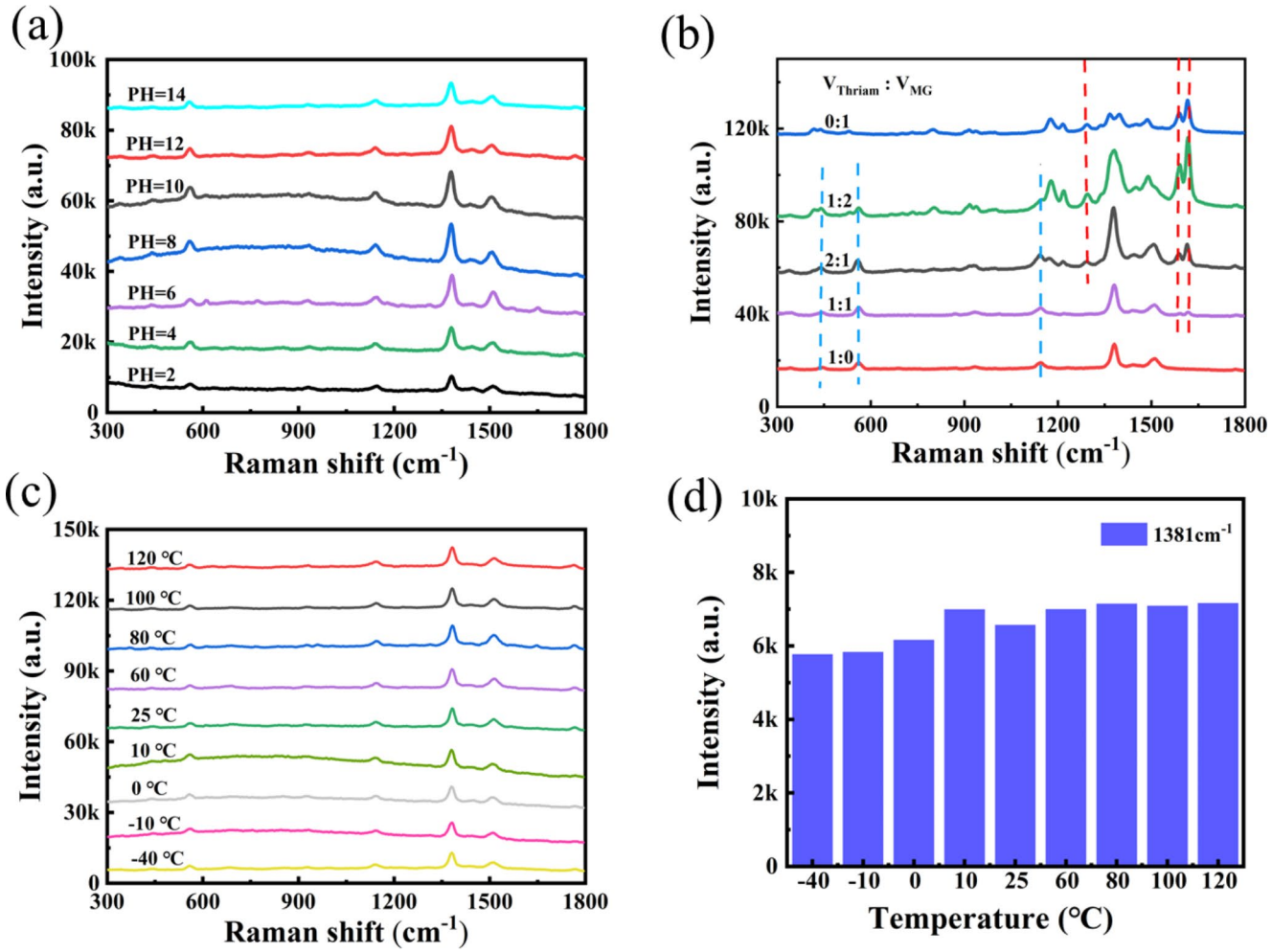

Fig. 7 (**a**) SERS spectra of 10^{-4} M thiram solution at various pH values. (**b**) SERS spectra of mixtures containing thiram and malachite green (MG) (The red line and blue line indicated the Raman peaks of MG and thiram, respectively). (**c**) SERS spectra of thiram adsorbed on the developed substrate at different temperatures. (**d**) Corresponding Raman intensity of thiram at 1381 cm^{-1} as a function of temperature

(MG), both at a concentration of 10^-4 M, were mixed in volume ratios of 1:1, 1:2 and 2:1. Then, the Raman peaks of thiram and malachite green were obviously measured on the developed substrate, as demonstrated in Fig. 7b. Moreover, the Ag NWs/M-CDG/PDMS substrate exhibited a wide operating temperature range. When the substrate was kept in -40°C freezer or placed in a drying cabinet at 120 °C, the SERS intensity remained within the ideal range, as shown in Fig. 7c-d. In a word, the Ag NWs/M-CDG/PDMS substrate had anti-corrosion properties, operated effectively over a broad temperature range, allowed for synchronous multi-analyte analysis, and resisted interference, making it highly suitable for diverse analytical applications.

2.10 Enhancement comparison under different illumination modes

A bidirectional excitation test was performed on the Ag NWs/M-CDG/PDMS substrate to evaluate its feasibility for in-situ analysis. Figure 8a illustrated concise models of the developed substrate under front-side and back-side illumination mode. Comparative SERS spectra of thiram solution with concentrations ranging from 10^{-4} to10^{-6} M were measured in both modes. As shown in Fig. 8b, the SERS spectra of thiram recorded from the front and the back sides of the prepared substrate were almost identical. This similarity can be attributed to the excellent transparency of the substrate, which allowed the incident laser and scattered light to pass through the medium unimpeded. Therefore, the fabricated Ag NWs/M-CDG/PDMS substrate was able to collect signals in back-side mode without attenuation of the electromagnetic enhancement. This developed substrate had

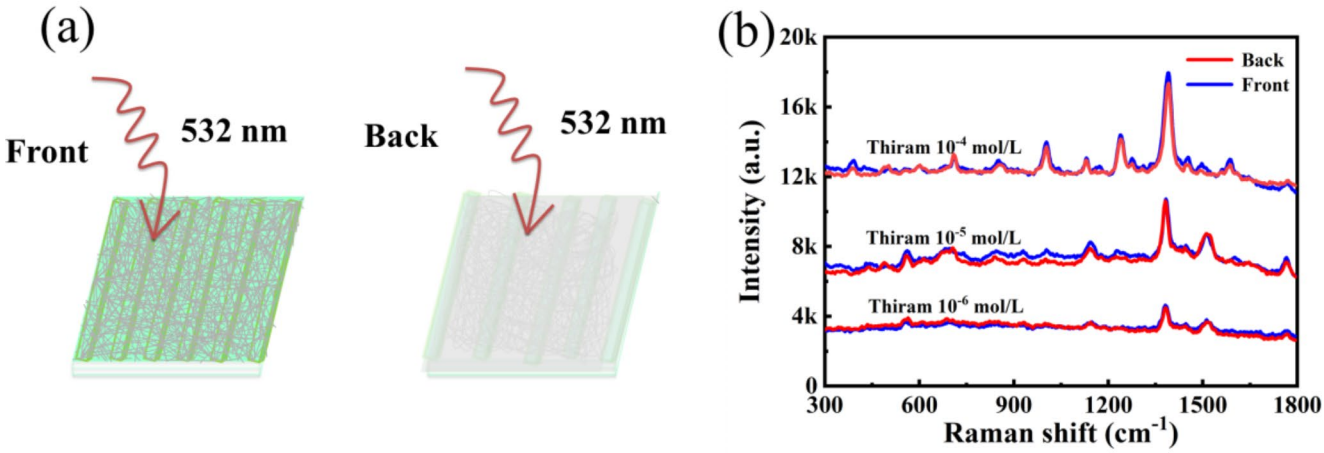

Fig. 8 (**a**) Schematic diagram of SERS measurements using front-side and back-side excitation. (**b**) Comparison of the SERS spectra of thiram (10^{-4}-10^{-6} M) recorded from the front and reverse sides of the Ag NWs/M-CDG/PDMS susbstrate

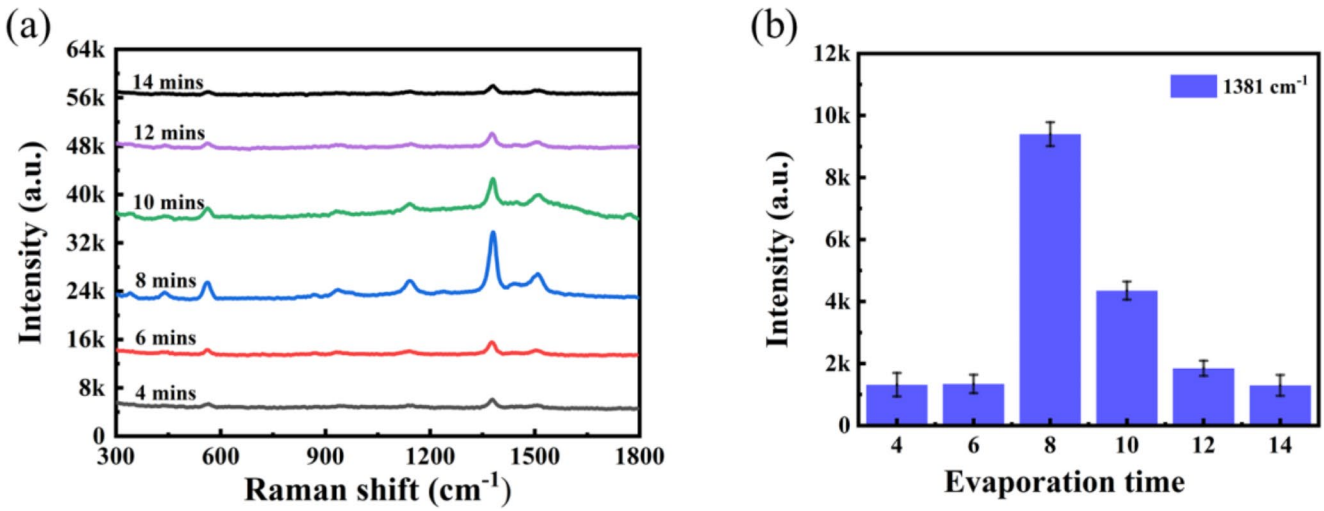

Fig. 9 (**a**) SERS spectra of thiram in the vapor phase on the substrate at different evaporation times of 4, 6, 8, 10, 12, and 14 min. (**b**) Corresponding Raman intensities at 1381 cm^{-1}

enormous potential for applications in the field of in-situ SERS detection.

2.11 The vapor phase testing on Ag NWs/M-CDG/PDMS substrate

Given that the Ag NWs/M-CDG/PDMS substrate exhibited high sensitivity, it was worthwhile to investigate its performance in vapor detection. However, research on SERS detection in the vapor phase is relatively scarce. Because molecules in the vapor phase possess higher kinetic energy compared to those in solid or liquid states, it is necessary for the Ag NWs/M-CDG/PDMS substrate to effectively capture and absorb probe molecules at the plasmonic "hot spots" of the SERS substrate.

0.01 g thiram powder was kept in small beaker. Then, the developed substrate was arranged at the opening of the small beaker, with the necessity of maintaining good air-tightness to ensure the integrity of the experiment. A series of small beaker containing of thiram powder were subjected to heating for durations of 4, 6, 8, 10, 12, and 14 min. As depicted in Fig. 9a, the SERS intensity of thiram initially increased with the evaporation time, reaching a peak at 8 min before declining. Figure 9b showed the corresponding Raman intensity of thiram at 1381 cm^{-1}, revealing that the most intense Raman signal occurred at an evaporation time of 8 min. It revealed that at an evaporation time of 8 min, the Raman signal of thiram was the intensest. The result could be attributed to the adsorption capacity of thiram vapor molecules on the Ag NWs/M-CDG/PDMS substrate. With increasing evaporation time, the adsorption number of

vapor molecules on the prepared substrate also increased. At 8 min, the substrate reached saturation in terms of adsorbed molecules, leading to the strongest Raman signal. Beyond this point, extending the evaporation time did not increase adsorption further, and thus the Raman signal would not continue to intensify.

3 Conclusions

A flexible Ag NWs/M-CDG/W-PDMS substrate with high sensitivity and good uniformity was designed and fabricated in this work. The grating-structured Ag NWs/PDMS substrate had a higher detection limit due to its unique structural design. Meanwhile, the introduction of APTES-treatment facilitated the deposition and stabilization of Ag NWs, thereby demonstrating highly sensitive SERS activity and better uniformity. In view of its good mechanical stability, corrosion resistance, capability for mixed analyte detection, wide operating temperature range and effectiveness in vapor phase detection, the Ag NWs/M-CDG/PDMS substrate as SERS substrate was well-suited for the detection of complex surfaces. In conclusion, this study proved that the Ag NWs/M-CDG/PDMS substrate had outstanding potential for highly sensitive and accurate on-site detection of pollutants in practical settings.

Supplementary Information The online version contains supplementary material available at https://doi.org/10.1007/s00339-024-08227-7.

Acknowledgements This research was supported by the National Natural Science Foundation of China (No. 22175119).

Author contributions Xinshuo Liu: Prepared the Ag NWs/M-CDG/PDMS substrates, analyzed the datas, and wrote the paper. Youchang Long: SEM and contact angle measurements. Lei Huang: Gave the theoretical guidance. Guina Xiao: Designed and supervised the research.

Declarations

Conflict of interest The authors declare that they have no known competing financial interests or personal relationships that could have appeared to influence the work reported in this paper.

References

1. A.F. Zhu, S. Ali, Y. Xu, Q. Ouyang, Q.S. Chen, Biosens. Bioelectron. **172**, 112806 (2021)
2. Y.W. Cheng, C.W. Hsiao, Z.L. Zeng, W.L. Syu, T.Y. Liu, Surf. Coat. Tech. **389**, 125653 (2020)
3. T.W. Xu, X.Q. Wang, X. Zhang, Z.C. Bai, Appl. Phys. A **128**, 317 (2022)
4. H.L. Zhao, W.W. Li, J. Li, Q.S. Yang, Y.H. Sun, M.T. Sun, Appl. Spectrosc. Rev. **59**, 224–246 (2024)
5. J.H. Yu, Y.N. Gao, W.Z. Zhang, P.J. Wang, Y. Fang, L.K. Yang, Spectrochimica Acta Part. A **317**, 124405 (2024)
6. Y.K. Chen, H. Li, J.M. Chen, D. Li, M.Y. Zhang, G.H. Yu, L. Jiang, Y. Zong, B. Dong, Z.F. Zeng, Y.D. Wang, L.F. Chi, Nano Res. **15**, 3496–3503 (2022)
7. Y.J. Yeh, C.Y. Liu, J.P. Chu, W.H. Chiang, K.L. Tung, Surf. Coat. Tech. **436**, 128285 (2022)
8. L. Liu, S.T. Hou, X.F. Zhao, C.D. Liu, Z. Li, C.H. Li, S.C. Xu, G.L. Wang, J. Yu, C. Zhang, B.Y. Man, Nanomaterials-Basel. **10**, 2371 (2020)
9. X.X. Li, X.Y. Duan, L. Li, S.J. Ye, B. Tang, Chem. Commun. **56**, 9320–9323 (2020)
10. A. Alyami, A.J. Quinn, D. Iacopino, Talanta. **201**, 58–64 (2019)
11. A.V. Markin, N.E. Markina, J. Popp, D. Cialla-May, Trac-Trend Anal. Chem. **108**, 247–259 (2018)
12. T.Y. Zhang, X.T. Li, D.M. Liu, J.Y. An, M.F. Zhang, J.H. Li, C.L. Jiang, Chem. Eng. J. **494**, 153082 (2024)
13. J. Lee, K. Min, Y. Kim, H.K. Yu, Materials. **12**, 1581 (2019)
14. K.C. Xu, R. Zhou, K. Takei, M.H. Hong, Adv. Sci. **6**, 1900925 (2019)
15. J.J. Wang, Z.H. Jia, C.W. Lv, Opt. Express. **26**, 6507–6518 (2018)
16. B. Bassi, B. Albini, A. D'Agostino, G. Dacarro, P. Pallavicini, P. Galinetto, A. Taglietti, Nanotechnology. **30**, 025302 (2019)
17. J. Chen, M.Z. Huang, L.L. Kong, M.S. Lin, Carbohyd Polym. **205**, 596–600 (2019)
18. D.S. Cheng, Y.L. Zhang, C.W. Yan, Z.M. Deng, X.N. Tang, G.M. Cai, X. Wang, J. Mol. Liq. **338**, 116639 (2021)
19. P. Kumar, R. Khosla, M. Soni, D. Deva, S.K. Sharma, Sens. Actuat B-Chem. **246**, 477–486 (2017)
20. M. Matamoros-Ambrocio, E. Sánchez-Mora, E. Gómez-Barojas, Polym. Compos. **15**, 2624 (2023)
21. Y. Li, J.W. Zhu, Y.Q. Ma, Y.H. Li, J. Shao, H.J. Li, J. Environ. Chem. Eng. **10**, 108916 (2022)
22. N. Yang, T.T. You, Y.K. Gao, C.M. Zhang, P.G. Yin, Spectrochimica Acta Part. A **202**, 376–381 (2018)
23. A.R. Paschoal, N.L.M. Costa, R.A. Domingues, E.B. Santos, Mater. Lett. **255**, 126557 (2019)
24. L.T. Guo, H.W. Cao, L.P. Cao, Y.F. Yang, M.L. Wang, Opt. Commun. **510**, 127921 (2022)
25. W.S. Yue, T.C. Gong, X.Y. Long, V. Kravets, P. Gao, M.B. Pu, C.T. Wang, Sens. Actuat B-Chem. **322**, 128563 (2020)
26. L.L. Lan, X.Y. Hou, Y.M. Gao, X.C. Fan, T. Qiu, Nanotechnology. **31**, 055502 (2020)
27. S. He, M.Y. Chang, P.C. Liu, X.Q. Wang, Z.C. Bai, Appl. Phys. A **126**, 953 (2020)
28. B.L. Chen, W. Zhou, M.S. Zhao, P.C. Si, Optik. **244**, 167537 (2021)
29. V. Sharma, S. Kumar, A. Jaiswal, V. Krishnan, Chemistryselect. **2**, 165–174 (2017)
30. J.W. Ba, Z.Z. Huang, W.S. Yang, Colloids Surf. A: Physicochem Eng. Aspects. **647**, 129033 (2022)